online data

The orphan transporter v7-3 (slc6a15) is a Na^+-dependent neutral amino acid transporter (B^0AT2)

Angelika BRÖER, Nadine TIETZE, Sonja KOWALCZUK, Sarah CHUBB, Michael MUNZINGER, Lasse K. BAK[1] and Stefan BRÖER[2]

School of Biochemistry & Molecular Biology, Australian National University, Canberra, ACT 0200, Australia

Transporters of the SLC6 (solute carrier 6) family play an important role in the removal of neurotransmitters in brain tissue and in amino acid transport in epithelial cells. In the present study, we demonstrate that mouse v7-3 (*slc6a15*) encodes a transporter for neutral amino acids. The transporter is functionally and sequence related to B^0AT1 (slc6a19) and was hence named B^0AT2. Leucine, isoleucine, valine, proline and methionine were recognized by the transporter, with values of $K_{0.5}$ (half-saturation constant) ranging from 40 to 200 μM. Alanine, glutamine and phenylalanine were low-affinity substrates of the transporter, with $K_{0.5}$ values in the millimolar range. Transport of neutral amino acids via B^0AT2 was Na^+-dependent, Cl^--independent and electrogenic. Superfusion of mouse B^0AT2-expressing oocytes with amino acid substrates generated robust inward currents. Na^+-activation kinetics of proline transport and uptake under voltage clamp suggested a 1:1 Na^+/amino acid co-transport stoichiometry. Susbtrate and co-substrate influenced each other's $K_{0.5}$ values, suggesting that they share the same binding site. A mouse B^0AT2-like transport activity was detected in synaptosomes and cultured neurons. A potential role of B^0AT2 in transporting neurotransmitter precursors and neuromodulators is proposed.

Key words: amino acid transport, B^0AT2, neurotransmitter transporter family, proline, solute carrier 6 (SLC6) transporter family, transport mechanism.

INTRODUCTION

Large neutral amino acids are frequently precursors for brain neurotransmitters. Aromatic amino acids are precursors for the neurotransmitters 5-hydroxytryptamine (serotonin), noradrenaline and dopamine. Branched-chain amino acids are important amino group donors for glutamate biosynthesis [1] and can serve as anaplerotic metabolites providing tricarboxylic acid cycle intermediates for glutamate and GABA (γ-aminobutyric acid) biosynthesis. It is often assumed that large neutral amino acids are transported into non-epithelial cells by the Na^+-independent system L amino acid transporter. However, in contrast with this notion, Na^+-dependent transport of large neutral amino acids has been described not only in epithelial cells, but also in a variety of brain cell preparations. Herrero et al. [2] reported Na^+-dependent uptake of tryptophan into vesicles derived from synaptosomes. Similarly, Yudkoff et al. [1] demonstrated Na^+-dependent uptake of leucine into synaptosomes. An Na^+-dependent transporter for large neutral amino acids with a similar substrate specificity as system L was also detected on the abluminal side of the blood–brain barrier [3]. These transporters are different from other well-known Na^+-dependent amino acid transporters, such as system ASC or system A, none of which transport branched-chain or aromatic acids [4].

The SLC6 (solute carrier 6) family is one of the largest transporter families in the human genome and currently comprises 20 members [5]. They are grouped into four subfamilies, namely the monoamine transporter branch, the GABA transporter branch, the amino acid transporter branch and the 'orphan transporter branch' [6]. We have recently identified the Na^+-dependent neutral amino acid transporter B^0AT1 (SLC6A19) [7], which is most closely related to the orphan transporters, suggesting that the orphans may in fact be amino acid transporters. This notion was subsequently reinforced by the identification of the Na^+- and Cl^--dependent IMINO transporter (SLC6A20), considered previously to be the orphan transporter XT3 or XTRP3 [8,9]. The orphan transporter v7-3 was initially cloned from rat brain [10], bovine brain [11] and human cerebellum [12], but no functional activity has been reported. The transporter failed to show active uptake of neurotransmitters, such as dopamine, noradrenaline, 5-hydroxytryptamine, GABA, glycine and glutamate, in two different expression systems [10]. In the present paper, we show that slc6a15, previously called neurotransmitter transporter v7-3 or NTT7-3, is a high-affinity Na^+-dependent transporter for large neutral amino acids. Because of its functional similarity to B^0AT1, we suggest naming the transporter B^0AT2.

MATERIALS AND METHODS

cDNA cloning and plasmids

Total RNA was isolated from mouse brain using the Nucleospin RNA kit (Macherey-Nagel, Düren, Germany). To clone mB^0AT2 (mouse B^0AT2), cDNA was synthesized as described previously [8]. The coding sequence was amplified using Pfu polymerase (Promega, Madison, WI, U.S.A.) during 40 PCR cycles of 95 °C, 30 s; 55 °C, 60 s; and 72 °C, 15 min using the sense primer, 5′-CCACC**ATG**CCTAAGAATAGCA-3′, and the antisense primer,

Abbreviations used: (Me)AIB, (*N*-methyl)aminoisobutyric acid; BCH, 2-aminobicyclo[2,2,1]heptane-2-carboxylic acid; mB^0AT2, mouse B^0AT2; EST, expressed sequence tag; GABA, γ-aminobutyric acid; HBSS, Hanks balanced salt solution; MCT1, monocarboxylate transporter 1; NMDG, *N*-methyl-D-glucamine; PAT1, proton amino acid transporter 1; PROT, proline transporter; RT, reverse transcription; SLC6, solute carrier 6; SNAT1, system N/A transporter 1.

[1] Present address: Department of Pharmacology, The Danish University of Pharmaceutical Sciences, 2 Universitetsparken, DK-2100 Copenhagen, Denmark.

[2] To whom correspondence should be addressed (email stefan.broeer@anu.edu.au).

The nucleotide sequence data reported will appear in DDBJ, EMBL, GenBank® and GSDB Nucleotide Sequence Databases under the accession number AM085111.

5′-CCCTGCTTTCGTTCAGCTAC-3′. The sense primer corresponds to bases 435–450 of the mouse cDNA NM_175328 (GenBank® accession number) and, in addition, contains a Kozak consensus sequence (underlined) in front of the start codon (in boldface). The antisense primer corresponds to bases 2621–2640 of the same cDNA. The B^0AT2 PCR product was purified by agarose gel electrophoresis, and the 2205 bp fragment was isolated using a gel elution kit (Qiagen, Clifton Hill, VIC, Australia). The isolated PCR fragment was initially cloned using the Zero Blunt TOPO PCR cloning kit (Invitrogen, Mulgrave, VIC, Australia); its sequence was confirmed (Biomolecular Resource Facility, Australian National University) and deposited under accession number AM085111 in the GenBank® database. For expression studies, mB^0AT2 was excised with HindIII/XbaI and inserted into the same sites of the oocyte expression vector pGEM-He-Juel [13].

Oocytes and injections

Oocyte isolation and maintenance have been described in detail previously [14]. For expression in oocytes, mB^0AT2 in pGem-He-Juel was linearized with SalI and transcribed *in vitro* using the T7 mMessage mMachine Kit (Ambion, Austin, TX, U.S.A.). Oocytes were injected with 30 ng of cRNA encoding mB^0AT2. Transport measurements were carried out after 3–10 days of expression. Rat MCT1 (monocarboxylate transporter 1) was used as described previously [15].

Cell culture

Neuron-rich primary cultures were derived from embryonic mouse brains as described by Brewer et al. [16]. Embryos were removed from the uteri of pregnant mice on E17 (embryonic day 17). Complete brains were prepared and stored in Ca^{2+}- and Mg^{2+}-free HBSS (Hanks balanced salt solution; 137 mM NaCl, 5.4 mM KCl, 0.44 mM KH_2PO_4, 2.7 mM Na_2HPO_4 and 10 mM Hepes) supplemented with pyruvate (1 mM) and 10 mM Hepes, pH 7.4 (storage solution). Cells were dissociated by passage through a 211 μm nylon mesh and resuspended in the storage solution (0.2 ml per brain) by triturating with a 1 ml automatic pipette. Cells were diluted to twice the original volume with the storage solution supplemented with Ca^{2+} (1.26 mM) and Mg^{2+} (0.9 mM) and collected by centrifugation at 200 ***g*** for 5 min. The pellet of cells from one litter (10–13 animals) was resuspended in 20 ml of Neurobasal/B27 (Invitrogen, Mulgrave, VIC, Australia) supplemented with 0.5 mM glutamine, 0.025 mM glutamate, 20 units/ml penicillin and 0.02 mg/ml streptomycin; 3×10^5 cells were seeded on to poly(D-lysine)-coated 35-mm-diameter dishes. Cells were incubated at 37 °C in a humidified atmosphere of 19:1 air/CO_2, in serum-free Neurobasal/B27 medium supplemented with 0.5 mM glutamine, 0.025 mM glutamate, 20 units/ml penicillin and 0.02 mg/ml streptomycin. Half of the medium was replaced by fresh medium without glutamate every fourth day. Transport experiments were carried out 9 days after seeding. To examine the purity of the cultures (Supplementary Figure 1 at http://www.BiochemJ.org/bj/393/bj3930421add.htm), cells were washed with PBS and then fixed for 10 min in 3.5 % (w/v) paraformaldehyde in PBS. Paraformaldehyde was removed by washing dishes twice with PBS and once with 0.1 % (w/v) glycine in PBS. As a preparation for staining, cells were permeabilized by treatment with 0.3 % (v/v) Triton X-100 in PBS for 10 min. Antigens were detected by incubation with primary and secondary antibodies in 10 % (v/v) goat serum in 0.1 % (w/v) PBS for 2 h each. A monoclonal anti-GFAP (glial fibrillary acidic protein) antibody (diluted 1:5; Dianova, Hamburg, Germany) and a polyclonal rabbit anti-(neurofilament 200) antibody (diluted 1:10; Sigma, St. Louis, U.S.A.) were used as primary antibodies. Phycoerythrin-labelled sheep $F(ab')_2$ anti-(mouse IgG) (Amrad Biotech, Richmond, VIC, Australia) or FITC-labelled goat anti-(rabbit IgG) (Sigma) were used as secondary antibodies.

Synaptosomes

Mouse cortical synaptosomes were prepared essentially as described by Lopez-Perez [17]. Briefly, the method employs differential centrifugation in a continuous sucrose gradient followed by a purification procedure based on a two-phase aqueous system of dextran 500 and PEG [poly(ethylene glycol)] 4000 [18]. The cerebral cortex of four to seven adult mice was used for each preparation. The purified synaptosomes were suspended to a final protein concentration of 0.5 mg/ml in a buffer solution (pH 7.4) containing 0.32 M sorbitol, 0.1 mM potassium EDTA and 5 mM potassium phosphate. The suspension was frozen rapidly in liquid nitrogen and stored at − 160 °C for up to 2 weeks. On the day of the experiment, the synaptosomal suspension was thawed at 37 °C and then maintained on ice for the duration of the experiment.

Flux measurements

Flux experiments in oocytes were performed as described previously [14]. ND96 (96 mM NaCl, 2 mM KCl, 1.8 mM $CaCl_2$, 1 mM $MgCl_2$ and 5 mM Hepes, titrated with NaOH to pH 7.4, unless otherwise indicated) was used as an incubation buffer. To achieve Na^+-free conditions, NaCl was replaced by NMDG (*N*-methyl-D-glucamine)-Cl or LiCl. To determine the Na^+-dependence of transport, NaCl-ND96 (pH 7.4) was mixed with NMDG-Cl-ND96 (pH 7.4, NaCl replaced by NMDG-Cl) in different proportions. Different pH values were adjusted by mixing Mes-buffered ND96 (5 mM Hepes replaced by 5 mM Mes) with Tris-buffered ND96 (5 mM Hepes replaced by 5 mM Tris base). Oocytes were depolarized by addition of 50 mM KCl. Uptake of [^{14}C]proline increased linearly with time for up to 20 min. As a result, uptake was determined using an incubation period of 10–15 min. All oocyte experiments were performed at least three times.

Transport experiments with primary cultures of neurons were performed at 37 °C. Growth medium was aspirated, and cells were washed three times with 2 ml of modified HBSS (bicarbonate-free, Hepes-containing HBSS: 136.6 mM NaCl, 5.4 mM KCl, 2.7 mM Na_2HPO_4, 1 mM $CaCl_2$, 0.5 mM $MgCl_2$, 0.44 mM KH_2PO_4 and 0.41 mM $MgSO_4$, containing 5 mM Hepes, pH 7.5). To initiate transport, 1.8 ml of modified HBSS containing [^{14}C]proline and unlabelled proline at a final concentration of 50 μM and a specific radioactivity of 120 kBq/nmol was added to the cells. Unlabelled competitive inhibitors were added at a final concentration of 5 mM. After 5 min, transport was stopped by aspirating the transport buffer, followed by three washing cycles with 2 ml of ice-cold modified HBSS. To determine Na^+-independent transport, NaCl was replaced by NMDG-Cl. Cells were lysed by addition of 1 ml of 0.1 M HCl. Of the resulting suspension, a 900 μl aliquot was mixed with 3 ml of scintillation cocktail (Ultima Gold; PerkinElmer Life and Analytical Sciences, Boston, MA, U.S.A.), and radioactivity was determined by liquid-scintillation counting. A portion of 100 μl was used for protein determination using the Bradford reagent (Sigma, Castle Hill, NSW, Australia).

To measure proline uptake in synaptosomes, 20 μl of synaptosomal suspension (8–10 μg of protein) was added to 180 μl of HBSS (1.26 mM $CaCl_2$, 5.4 mM KCl, 0.4 mM KH_2PO_4, 0.5 mM $MgCl_2$, 0.4 mM $MgSO_4$, 136.6 mM NaCl or NMDG-Cl, 10 mM Hepes and 2.7 mM Na_2HPO_4, pH 7.5) at room temperature (23 °C), which generates a large inwardly directed

Table 1 Primers used to amplify proline transporters in RT–PCR

All sequences are from mouse. F, forward; R, reverse; fragment size in parentheses.

Primer	Sequence
B^0AT2 (1387 bp)	F, 5′-CCCATACCTCTGCCAAAAGA-3′ R, 5′-TGCCATAAACAAAGCTCACG-3′
SNAT1 (400 bp)	F, 5′-ACAGGCGACATTCTCATCCT-3′ R, 5′-CAGAGGAGCAAGCCCAGTC-5′
SNAT2 (417 bp)	F, 5′-TGGGGCTATGTCAAGCTACC-3′ R, 5′-AACGTCAGGATGGGTACTGC-3′
PAT1 (386 bp)	F, 5′-ATGGGGACACGGTGATGTAT-3′ R, 5′-TCTGGGATCCTCTGGACAA-3′
PROT (489 bp)	F, 5′-CTGCTGATGACTCCCAGTGA-3′ R, 5′-CAGCACCCCATTACCACTCT-3′
PAT2 (454 bp)	F, 5′-ACTGGCTTTCAGTCCCAAT-3′ R, 5′-CACACCGATGCTTTCAAAT-3′

Na^+-gradient. To determine Na^+-independent uptake, NaCl was replaced by NMDG-Cl. The synaptosomes were allowed to accumulate substrate for 5 min in the presence of 50 μM L-proline and 3.7 kBq of L-[^{14}C]proline in the absence or presence of a 200-fold excess (10 mM) of competing substrates. The uptake was terminated by adding 2 ml of ice-cold buffer containing 5 mM unlabelled proline to the transport assay. Synaptosomes were collected on nitrocellulose filters (0.45 μm pore size) and accumulated radioactivity was measured using liquid-scintillation counting.

Electrophysiological recordings

Amino-acid-induced currents were analysed by two-electrode voltage clamp recording. The recordings were performed with $1 \times$ LU and $10 \times$ MGU headstages connected to a Geneclamp 500B electronic amplifier (Axon Instruments, Union City, CA, U.S.A.). The output signal was amplified 10-fold and filtered at 50 Hz. The analogue signal was converted by a Digidata 1322A (Axon Instruments), and data were sampled using pCLAMP software (Axon Instruments). Oocytes were chosen that had a membrane potential more negative than -30 mV. Once a stable membrane potential was reached under current-clamp conditions, the amplifier was switched to voltage-clamp mode, holding the oocytes at -50 mV. ND96 was used as control solution in all recordings. A complete change of the bath to a new solution was accomplished in approx. 10 s. During steady-state measurements, data were sampled at 3 Hz. To study voltage-dependence of the transporter, the holding potential was increased stepwise from -150 mV to $+50$ mV in increments of 10 mV; the step length was 500 ms and the sampling rate was increased accordingly. To determine the stoichiometry of B^0AT2, the flow-through of ND96 was stopped and 20 μl of 10 mM [^{14}C]proline was added to the bath, giving a final concentration of 1 mM. After 15 min, the flow-through was restarted to remove the radioactive substrate. After the inward current ceased, the oocyte was removed and placed in a scintillation vial to determine its radioactivity. The amount of accumulated radioactivity was compared with that of the integrated inward current.

RT (reverse transcription)–PCR

RT–PCR was performed as described previously [8] using RNA isolated from mouse tissues or cultured mouse neurons. The primers shown in Table 1 were used to amplify mouse proline transporters.

A 1-kb actin cDNA fragment was amplified as a control during 30 cycles using the following primers: 5′-GCTCACCATGGATGATATCGC-3′ and 5′-GGAGGAGCAATGATCTTGATCTTC-3′.

Calculations, statistics and computer analysis

Each datapoint or column in the Figures, Table 2 and Table 3 represents the activity (mean $\pm$ S.D.) for seven to ten mB^0AT2-expressing oocytes. In flux experiments, the activity (mean $\pm$ S.D.) of seven to ten non-injected oocytes was subtracted from this activity. Flux studies in cells and synaptosomes were performed in triplicate. Kinetic constants were derived by non-linear curve-fitting using Origin7.0 software (OriginLab Corporation, Northampton, MA, U.S.A.). To determine $K_{0.5}$ (half-saturation constant) and I_{max} (maximum current), the Michaelis–Menten equation:

$$I = \{I_{max} \times [S]/(K_{0.5} + [S])\}$$

or the Hill equation:

$$I = \{I_{max} \times [S]^h/(K_{0.5}^h + [S]^h)\}$$

were used, where h is the Hill coefficient, I is actual current and [S] is substrate concentration. Sequence alignment was calculated using programs of GCG and PHYLIP packages supplied by ANGIS (Australian National Genomic Information Service). Sequence alignment was performed using ClustalW [19].

RESULTS

Cloning of mB^0AT2 (v7-3)

The SLC6 family comprises transporters for monoamines, GABA, taurine, creatine and amino acids in addition to a large group of orphan transporters. We showed recently that two orphan transporters, namely SLC6A19 (B^0AT1) and SLC6A20 (IMINO), are amino acid transporters [7,8]. Subsequently, we wanted to test the hypothesis that other members of the orphan transporter branch are also amino acid transporters. To this end, we amplified the *slc6a15* sequence from mouse brain and deposited its sequence under accession number AM085111 in the GenBank® database. The transcript encodes a membrane protein of 729 amino acids in length. Alignment with the other mouse members of the SLC6 family reveals that mB^0AT2 is more closely related to NTT4 (slc6a17) than it is to mB^0AT1. mB^0AT2 shares 65 % identical amino acids with mNTT4 but shows only 35 % identity with mB^0AT1 (slc6a19), XT2 (slc6a18) and IMINO (slc6a20), with all other SLC6 family members having between 21 % and 35 % identity with mB^0AT2.

Substrate specificity of mB^0AT2 (v7-3)

Expression of mB^0AT2 in *Xenopus laevis* oocytes resulted in a significant increase of neutral-amino acid uptake activity compared with control oocytes. Significant uptake above non-injected oocytes was observed for proline, leucine, isoleucine, alanine and phenylalanine (Figure 1A). Because there is negligible endogenous proline uptake in oocytes, we determined the substrate specificity of B^0AT2 by challenging the uptake of 50 μM [^{14}C]proline with a 100-fold excess of unlabelled L-amino acids (Figure 1B). Proline uptake was strongly (>90 %) inhibited by methionine, leucine, isoleucine, valine, proline, alanine and the amino acid analogue AIB (aminoisobutyric acid). Partial inhibition (40–90 %) was exerted by phenylalanine, serine, threonine, glutamine, asparagine, histidine, hydroxyproline and by the amino acid analogues BCH (2-aminobicyclo[2,2,1]heptane-2-carboxylic acid) and nipecotic acid. No significant inhibition was observed on addition of glycine, tyrosine, tryptophan, cysteine,

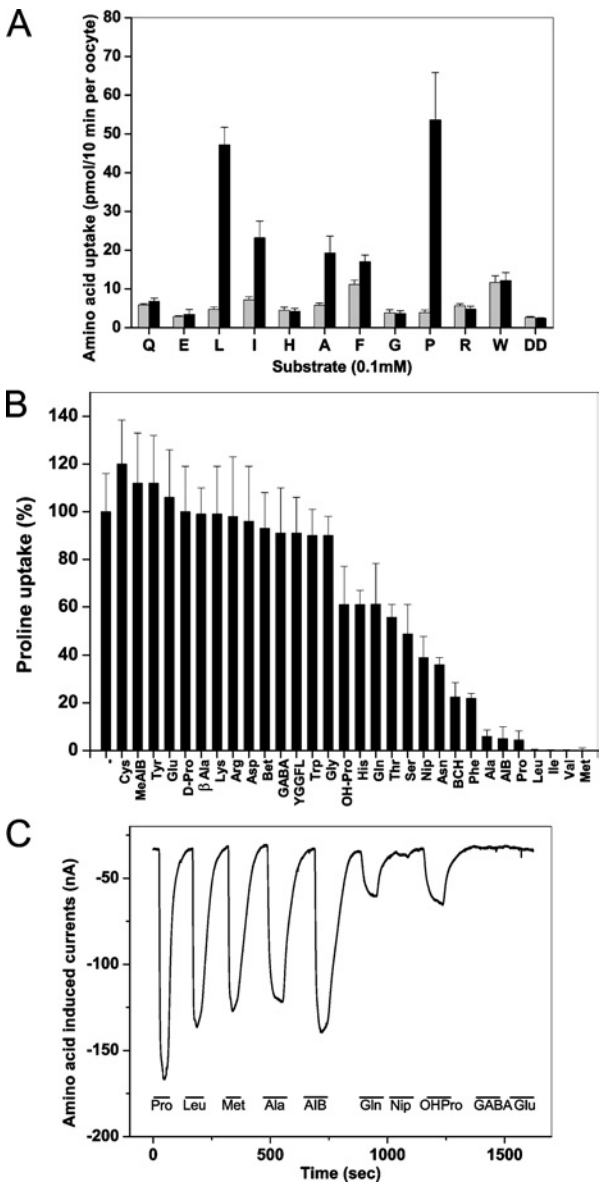

Figure 1 Substrate specificity of mB^{0}AT2

(**A**) Uptake of [^{14}C]glutamine, [^{14}C]glutamate, [^{14}C]leucine, [^{14}C]isoleucine, [^{14}C]histidine, [^{14}C]alanine, [^{14}C]phenylalanine, [^{14}C]glycine, [^{14}C]proline, [^{14}C]arginine, [^{3}H]tryptophan and D-[^{3}H]aspartate (DD), each 100 μM, was determined 4 days after injection. Each bar represents the transport activity (mean $\pm$ S.D.) of ten oocytes (one of three similar experiments shown). Black bars represent the activity of mB^{0}AT2-expressing oocytes, and grey bars represent the transport activity of non-injected oocytes. (**B**) [^{14}C]proline uptake (50 μM) was determined 4–6 days after injection in the presence or absence of 5 mM of unlabelled amino acids, their analogues or 0.1 mM [leucine]enkephalin. Each bar represents the transport activity (mean $\pm$ S.D.) of ten oocytes. Data are compiled from three different experiments. The transport activity of non-injected oocytes was subtracted in each case. (**C**) Oocytes were each injected with mB^{0}AT2 cRNA or remained uninjected in the controls. After incubation for 5 days, oocytes were held at a membrane potential of -50 mV and superfused with ND96 (pH 7.4) alone or ND96 (pH 7.4) containing different amino acids at a final concentration of 1 mM. Superfusion with amino-acid-containing solutions is indicated by bars. Non-injected oocytes showed inward currents of 2–3 nA in response to the same panel of amino acids. β Ala, β-alanine; Bet, betaine; Nip, nipecotic acid; OH-Pro, hydroxyproline; YGGFL, [leucine]enkephalin. One-letter or three-letter codes are used for amino acids.

arginine, lysine, aspartate or glutamate. A number of amino-acid-related compounds such as MeAIB [(*N*-methyl)AIB], β-alanine, GABA, betaine and [leucine]enkephalin (100 μM) also did not inhibit [^{14}C]proline uptake. In summary, it appears that large

Table 2 Substrate specificity of mB^{0}AT1 and mB^{0}AT2

Oocytes were each injected with 30 ng of mB^{0}AT1 or mB^{0}AT2 cRNA. Amino-acid-induced currents were determined 3–6 days after injection, by discharging substrate-containing solutions directly into the bath, close to the oocyte surface. Substrates were used at the concentration (in mM) indicated in parentheses. Currents are given relative to $I_{proline}$ (mB^{0}AT2) or $I_{leucine}$ (mB^{0}AT1); these reference currents are shown in bold. The amino-acid-induced currents (rows 1–20) in the mB^{0}AT1 column are taken from [20].

	Normalized current (%)	
Substrate	mB^{0}AT2	mB^{0}AT1
Proline	**100 $\pm$ 0** (1)	29 $\pm$ 1 (10)
Alanine	87 $\pm$ 10 (1)	56 $\pm$ 17 (10)
Valine	81 $\pm$ 10 (1)	95 $\pm$ 5 (10)
Methionine	76 $\pm$ 11 (1)	102 $\pm$ 10 (10)
Leucine	74 $\pm$ 11 (1)	**100 $\pm$ 0** (10)
Isoleucine	59 $\pm$ 2 (1)	97 $\pm$ 8 (10)
Threonine	46 $\pm$ 13 (1)	34 $\pm$ 3 (10)
Asparagine	38 $\pm$ 5 (1)	65 $\pm$ 9 (10)
Serine	38 $\pm$ 11 (1)	45 $\pm$ 7 (10)
Phenylalanine	33 $\pm$ 4 (1)	58 $\pm$ 12 (10)
Glutamine	24 $\pm$ 10 (1)	70 $\pm$ 7 (10)
Lysine	12 $\pm$ 4 (1)	10 $\pm$ 8 (10)
Glycine	12 $\pm$ 7 (1)	39 $\pm$ 13 (10)
Histidine	9 $\pm$ 4 (1)	30 $\pm$ 8 (10)
Arginine	6 $\pm$ 1 (1)	4 $\pm$ 4 (10)
Tryptophan	6 $\pm$ 2 (1)	19 $\pm$ 4 (10)
Tyrosine	3 $\pm$ 3 (1)	39 $\pm$ 9 (10)
Aspartate	3 $\pm$ 3 (1)	0.5 $\pm$ 1 (10)
Glutamate	0.5 $\pm$ 1 (1)	2 $\pm$ 2 (10)
Cysteine	0 $\pm$ 0 (1)	59 $\pm$ 12 (10)
5-Hydroxytryptamine	9 $\pm$ 7 (0.1)	0 $\pm$ 0 (0.1)
Glycine	6 $\pm$ 3 (0.1)	14 $\pm$ 4 (0.1)
Betaine	4 $\pm$ 2 (0.1)	7 $\pm$ 7 (0.1)
Noradrenaline	4 $\pm$ 3 (0.1)	4 $\pm$ 5 (0.1)
Creatine	4 $\pm$ 4 (0.1)	8 $\pm$ 7 (0.1)
Taurine	4 $\pm$ 3 (0.1)	7 $\pm$ 6 (0.1)
GABA	1 $\pm$ 1 (0.1)	0 $\pm$ 0 (0.1)
Dopamine	1 $\pm$ 1 (0.1)	0 $\pm$ 0 (0.1)

aliphatic neutral amino acids plus proline were the preferred substrates of mB^{0}AT2. The transporter was stereospecific, as indicated by the lack of inhibition of L-proline transport by D-proline (Figure 1B). The basic characteristics of mB^{0}AT2 as determined using flux experiments were confirmed by electrophysiological recordings of substrate-induced transporter currents (Figure 1C and Table 2). When tested at a concentration of 1 mM, currents were induced in the following order: Pro > Leu = Met = Ala = Val = AIB > Ile > Thr > Asn = Ser > Phe > Gln, confirming the order of transport activity as determined with labelled amino acids. All other amino acids tested did not elicit significant currents (Table 2). mB^{0}AT2 is functionally related and sequence-related to mB^{0}AT1 [20] but has a more restricted substrate specificity (Table 2). Neither mB^{0}AT1 nor mB^{0}AT2 accepted neurotransmitters or other substrates of SLC6 family members, such as taurine, creatine or betaine (Table 2). Two groups of mB^{0}AT2 substrates were identified. The high-affinity substrates (methionine, isoleucine, leucine and proline) were transported with apparent $K_{0.5}$ values of 40–200 μM (Table 3), whereas the low-affinity substrates (alanine, phenylalanine, glutamine and pipecolic acid) were transported with millimolar values of $K_{0.5}$ (Table 3).

Transport mechanism of mB^{0}AT2 (v7-3)

Uptake of [^{14}C]proline was Na^+-dependent; replacement of NaCl by NMDG-Cl completely abolished the transport activity, and

Table 3 Kinetic constants of neutral amino acid transport by mB^0AT2

Oocytes were each injected with 30 ng of mB^0AT2 cRNA or remained uninjected in the controls. Amino-acid-induced currents were determined 3–6 days after injection at concentrations ranging between 0.1 and 20 mM. The $K_{0.5}$ value in the table is the average for 12 oocytes from three oocyte batches.

Substrate	$K_{0.5}$ (μM)
Proline	195 ± 16
Leucine	81 ± 9
Isoleucine	58 ± 10
Methionine	40 ± 4
Alanine	670 ± 92
Phenylalanine	1050 ± 112
Glutamine	5300 ± 2700
Pipecolic acid	900 ± 200

replacement by LiCl reduced the transport activity by 80 % (Figure 2A). Similar to the properties of B^0AT1 [7], replacement of Cl^- with gluconate did not reduce the transport activity of B^0AT2. Addition of 50 mM KCl to the transport buffer, a manipulation that reduces the membrane potential of oocytes from -40 ± 7 mV to -16 ± 3 mV, reduced proline uptake by 43 % (Figure 2A). Addition of 100 mM sucrose did not change proline uptake significantly, suggesting that the inhibitory effect of KCl was not caused by the increased osmolarity (Figure 2A). This result confirmed that transport of amino acids via mB^0AT2 was indeed electrogenic, suggesting that the inward currents were coupled to amino acid transport and were not generated by a transport-associated ion conductance [21]. A coupling of substrate transport to Na^+-translocation was supported further by the voltage-dependence of proline-induced currents, which remained inwardly directed at all holding potentials tested (Figure 2B). To determine the number of charges translocated together with each substrate molecule, we determined [^{14}C]proline uptake under voltage-clamp conditions. A plot of the integrated current against accumulated [^{14}C]proline indicated a stoichiometry of 0.65 ± 0.07 charges/proline (Figure 2C). Transport of proline via mB^0AT2 was also dependent on extracellular pH, increasing with alkalinity (Figure 3A). The strong pH-dependence may point to a proton antiport mechanism. To test this possibility, we modulated the intracellular pH by coexpression of MCT1 [15]. Co-expression of MCT1 and B^0AT2 did not change the expression levels of the two transporters significantly (Figure 3B). Addition of 20 mM lactate to the oocytes, a manipulation that decreases the intracellular pH by approx. 0.7 pH unit [15], did not alter [^{14}C]proline uptake by B^0AT2, suggesting that the pH-dependence of B^0AT2 was caused by an exofacial pH-modifier site and not by a participation of protons in the transport mechanism.

An activation analysis of proline uptake as a function of the Na^+ concentration showed a hyperbolic dependence, suggesting that only one Na^+ ion is co-transported with proline (Figure 4A). Hill coefficients varied between 0.6 ± 0.2 and 1.0 ± 0.2, but were never > 1. To characterize the interaction between Na^+ and proline further, we determined kinetic constants at different substrate and co-substrate concentrations. When measured at a substrate concentration of 100 μM, half-maximal transport velocity was reached at a Na^+ concentration of 16 ± 4 mM (Figure 4A). However, the $K_{0.5}$ of Na^+ decreased significantly to 4.5 ± 0.7 and 2.8 ± 0.4 mM when increasing the proline concentration to 0.5 mM and 5 mM respectively (Figure 4A). The Na^+ concentration also affected the $K_{0.5}$ of proline. At 100 mM NaCl, proline was transported with a $K_{0.5}$ of 195 ± 10 μM. This value

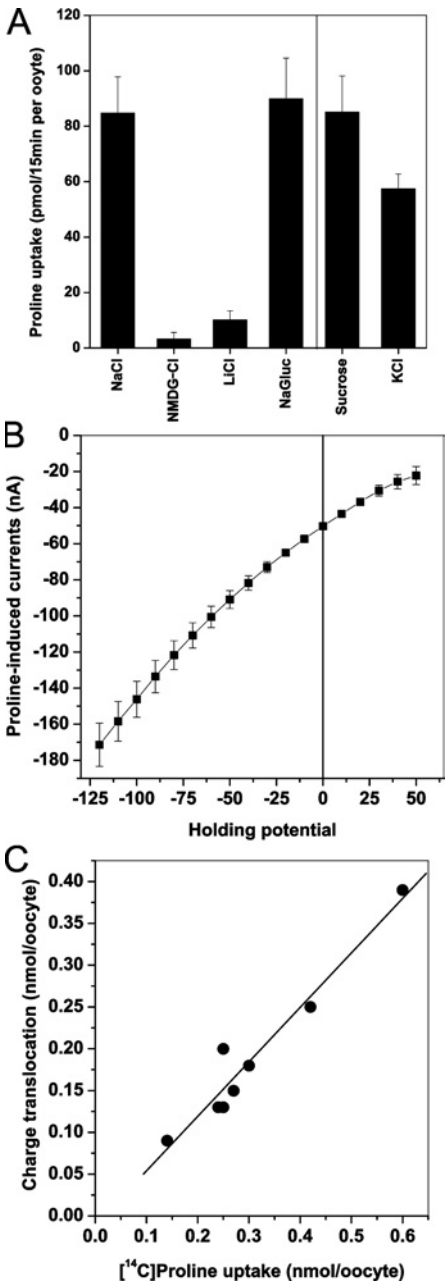

Figure 2 Ion-dependence, voltage-dependence and stoichiometry of amino acid uptake via mB^0AT2

Oocytes were each injected with mB^0AT2 cRNA or remained uninjected in the controls. (**A**) [^{14}C]Proline (100 μM) uptake was determined 5 days after injection, either in buffer containing NaCl or in buffer where NaCl was replaced by LiCl, NMDG-Cl or sodium gluconate (NaGluc). To investigate whether mB^0AT2 is electrogenic, [^{14}C]proline uptake (100 μM) was determined in ND96 buffer (pH 7.4) with or without addition of 50 mM KCl. These experiments were compared with a control with 100 mM sucrose added to ND96 (pH 7.4) balancing for the increased osmolarity. Each bar represents the transport activity (mean $\pm$ S.D.) of ten oocytes. The transport activity of non-injected oocytes was subtracted. One of three similar experiments is depicted. (**B**) Oocytes expressing mB^0AT2 cRNA were incubated for 5 days and subsequently superfused with 1 mM proline at a holding potential of -50 mV. After a stable inward current was established, the holding potential was varied between -120 mV and $+50$ mV in steps of 10 mV. The curve represents the means $\pm$ S.D. for seven oocytes. The experiment was performed three times with similar results. (**C**) Oocytes were each injected with mB^0AT2 cRNA. [^{14}C]Proline (1 mM) uptake was determined 6 days after injection in oocytes held at a potential of -50 mV. After incubation for 15 min, proline-induced currents were integrated and compared with the accumulation of [^{14}C]proline. The proline accumulation of eight individual oocytes is presented on the ordinate and plotted against the integrated inward current on the abscissa. Oocytes from three different batches were used for the experiment.

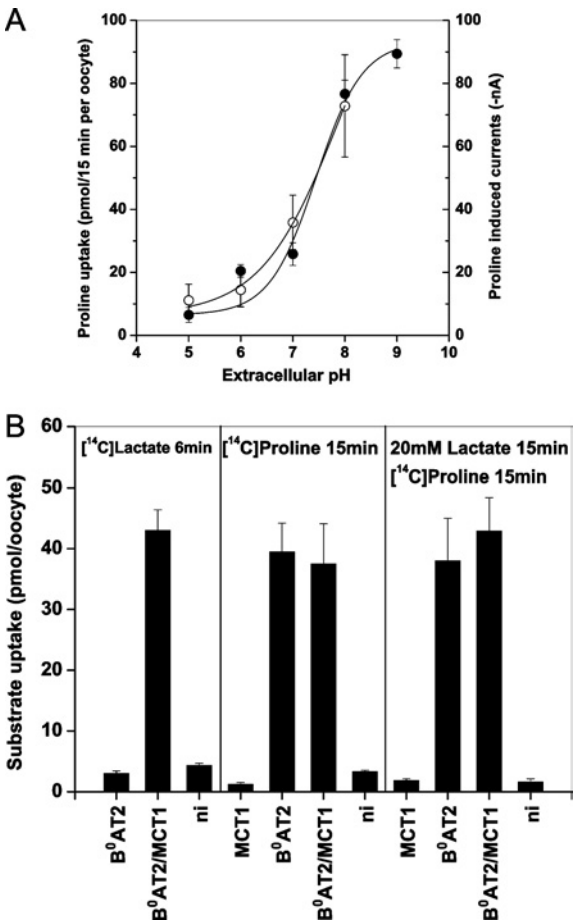

Figure 3 Intracellular and extracellular pH-dependence of proline transport via mB^{0}AT2

(**A**) [^{14}C]Proline uptake (100 μM, ●) was determined at pH values ranging from 5.0 to 9.0 in ND96 buffer containing 96 mM NaCl. Each datapoint represents the transport activity (mean ± S.D.) of ten oocytes. The transport activity of non-injected oocytes was subtracted. In a separate series of experiments (○) oocytes were held at −50 mV and superfused with proline-containing solutions (100 μM) at pH values ranging from 5.0 to 8.0. The inward currents (means ± S.D.) of seven oocytes are shown. The experiment was performed three times with similar results. (**B**) Oocytes were each injected with mB^{0}AT2 cRNA (23 ng), rMCT1 (rat MCT1) cRNA (10 ng) or rMCT1 (10 ng) plus mB^{0}AT2 (23 ng) cRNA, or remained uninjected (ni) in the controls. Uptake of L-[^{14}C]lactate (100 μM, left-hand panel) and [^{14}C]proline (100 μM, middle panel) was studied in oocytes expressing rMCT1, mB^{0}AT2 or rMCT1 plus mB^{0}AT2, and in non-injected oocytes, to demonstrate active expression of the two transporters. To investigate the effect of intracellular acidification, cytosolic pH was decreased by incubation with 20 mM lactate for 15 min at pH 7.0. Subsequently, [^{14}C]proline uptake was studied in the continued presence of 20 mM lactate for 15 min (right-hand panel).

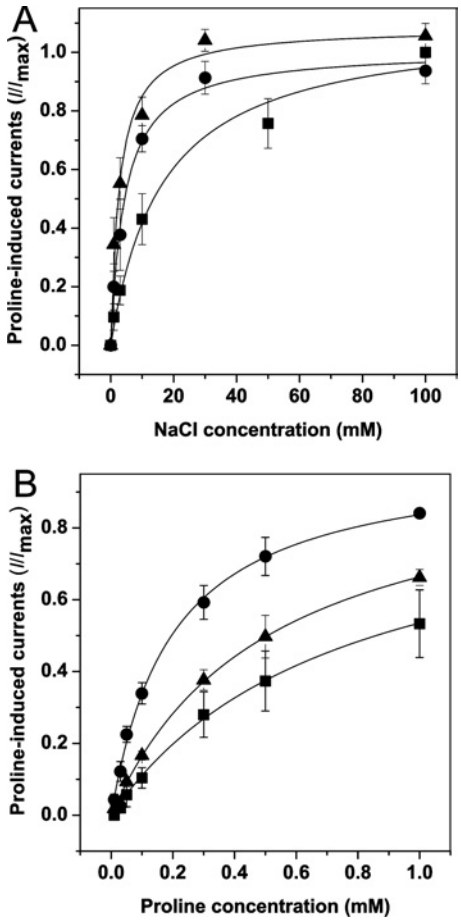

Figure 4 Kinetic parameters of proline transport and Na$^+$-activation kinetics

Oocytes were injected with 30 ng of mB^{0}AT2 cRNA. After 4–6 days of expression, the $K_{0.5}$ of Na$^+$-activation (**A**) was determined at proline concentrations of 0.1 mM (■), 0.5 mM (●) and 5 mM (▲). Each curve represents the mean ± S.D. of ten oocytes from three different oocyte batches. In a second set of experiments (**B**), the $K_{0.5}$ of proline was determined in the presence of 3 mM NaCl (■), 30 mM NaCl (▲) or 100 mM NaCl (●). Currents were normalized to the extrapolated V_{max} of each individual oocyte. Each curve represents the mean ± S.D. of ten oocytes from three different oocyte batches.

increased to 510 ± 40 μM and 740 ± 90 μM when the NaCl concentration was decreased to 30 mM and 3 mM respectively (Figure 4B). These results suggest that substrate and co-substrate influence each other's binding. The kinetic parameters of substrate and co-substrate also depended on the holding potential. When changing the holding potential from −80 mV to +20 mV, the $K_{0.5}$ value of proline changed from approx. 0.2 mM to 0.8 mM (Figure 5A). The calculated I_{max} increased linearly over this range of the electrical driving force (Figure 5B). The $K_{0.5}$ value (determined at a proline concentration of 0.1 mM) of Na$^+$ changed from 8.7 ± 0.4 mM to 19 ± 2 mM and > 50 mM when the holding potential was changed from −100 mV to −50 mV and −10 mV respectively (Figure 5C).

Tissue distribution of mB^{0}AT2 (v7-3)

RT–PCR experiments showed significant expression of mB^{0}AT2 only in brain, lung and kidney (Figure 6). Expression of mB^{0}AT2 was abundant in all three major brain regions, namely the cortex, the cerebellum and the brain stem. The RT–PCR data were confirmed by analysis of the EST (expressed sequence tag) database. Of 74 ESTs corresponding to NM_175328 shown in the Unigene database, 45 are found in the brain and 22 are found in the eye. Between one and three ESTs were detected in mammary gland, kidney, skin and testis. Transcripts of mB^{0}AT2 were detected throughout development, starting with the pre-implantation embryo.

Proline uptake in cultured neurons and synaptosomes

The transport activity of mB^{0}AT2 demonstrates its expression at the oocyte cell surface. To determine whether mB^{0}AT2 is also expressed in the plasma membrane of neural cells, we characterized proline transport in cultured neurons and synaptosomes. Uptake of [^{14}C]proline (50 μM) in cultured neurons was entirely Na$^+$-dependent. Marginal proline uptake was observed when

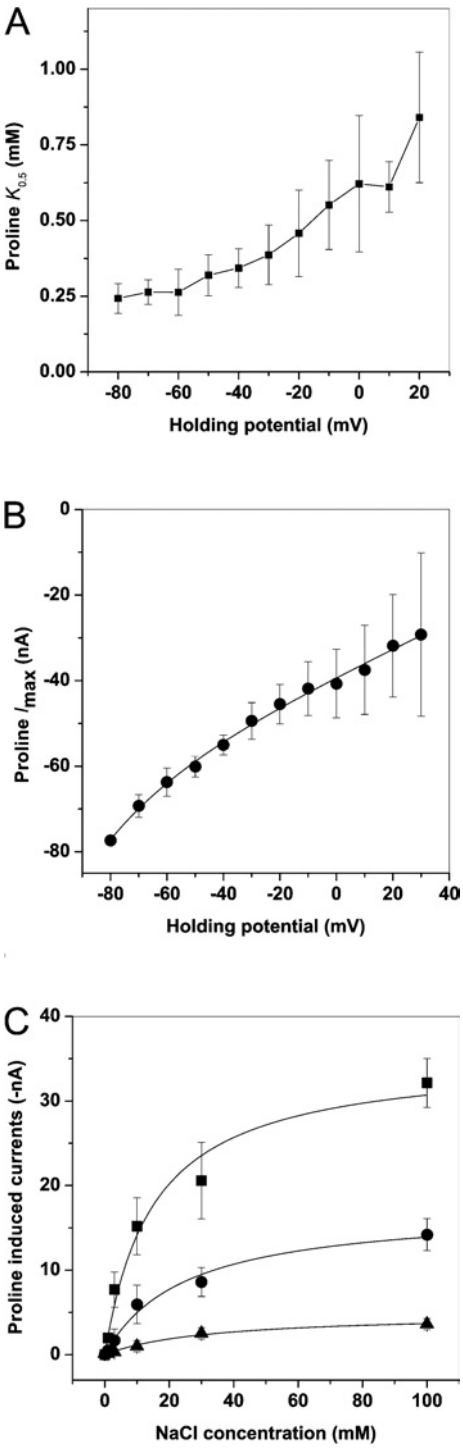

Figure 5 Voltage-dependence of kinetic parameters

Oocytes were injected with mB^0AT2 cRNA. After 5 days, oocytes were superfused with ND96 (pH 7.4) alone or ND96 (pH 7.4) containing proline concentrations of 0.01 mM, 0.03 mM, 0.1 mM, 0.3 mM or 1 mM. After reaching steady-state currents, the holding potential was varied between -80 mV and $+30$ mV in steps of 10 mV to derive $K_{0.5}$ values (**A**) and I_{max} values (**B**) at different holding potentials. Each datapoint represents the transport activity (mean $\pm$ S.D.) of ten oocytes. The experiment was performed three times with similar results. (**C**) Oocytes were each injected with 30 ng of mB^0AT2 cRNA. After incubation for 5 days, oocytes were superfused with ND96 (pH 7.4) or with ND96 where NaCl was replaced with NMDG-Cl to give the indicated concentration. Inward currents were induced by 0.1 mM proline. The holding potential was -10 mV (■), -50 mV (●) or -100 mV (▲). Each datapoint represents the mean $\pm$ S.D. for ten oocytes. The experiment was performed three times with similar results. Error bars, when not visible, were smaller than the symbol of the datapoint.

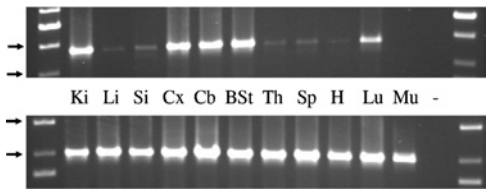

Figure 6 RT–PCR analysis of mB^0AT2 mRNA in mouse tissues

Total RNA was isolated from different mouse tissues and reverse-transcribed into cDNA. In a control reaction, cDNA was omitted (−). Upper panel: mB^0AT2-specific fragment of 1387 bp. Lower panel: equal loading was tested by amplifying an actin-specific fragment in the same tissue samples. Markers were loaded on each side of the gel; arrows indicate bands of 1000 bp and 1500 bp. Ki, kidney; Li, liver; Si, small intestine; Cx, brain cortex; Cb, brain cerebellum; BSt, brain stem; Th, thymus; Sp, spleen; H, heart;. Lu, lung; Mu, muscle.

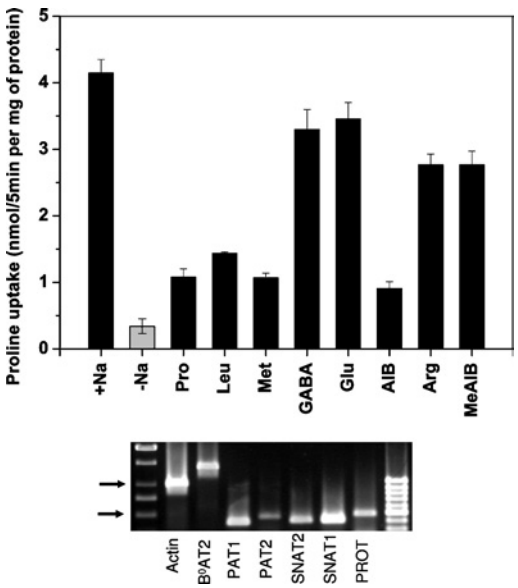

Figure 7 Proline transport in cultured neurons

(**A**) Uptake of [^{14}C]proline (50 μM) was determined over a time period of 5 min at 37 °C in primary cultures of neurons in the presence (black bars) or absence (grey bar) of Na^+. In the presence of Na^+, [^{14}C]proline uptake was challenged with 5 mM unlabelled amino acids, MeAIB or AIB. (**B**) Total RNA was isolated from cultured neurons, and the proline transporters B^0AT2, PAT1, PAT2, SNAT2, SNAT1 and PROT were detected by RT–PCR. Actin was used as a control. DNA markers of 500 bp and 1000 bp are indicated by arrows.

NaCl was replaced by NMDG-Cl (Figure 7A). In the presence of Na^+, proline uptake was strongly inhibited by a 100-fold excess of the B^0AT2 substrates leucine, alanine, AIB and proline itself. Other amino acids or related compounds, which are not substrates of B^0AT2, such as MeAIB, GABA, arginine or glutamate, inhibited proline transport only slightly. Using RT–PCR, six proline transporters were detected in cultured neurons, namely the system A isoforms SNAT1 (system N/A transporter 1) and SNAT2 [22], the proton amino acid transporters PAT1 (proton amino acid transporter 1) and PAT2 [23], the neuronal proline-specific transporter PROT (proline transporter) [24] and B^0AT2 (Figure 7B). The cultures contained less than 3% astrocytes (Supplementary Figure 1 at http://www.BiochemJ.org/bj/393/bj3930421add.htm), arguing against a contribution of other cell types to proline uptake.

A [leucine]enkephalin-sensitive proline transporter has been described in synaptosomes as having similar properties to the proline-specific transporter PROT (slc6a7) [25]. Since

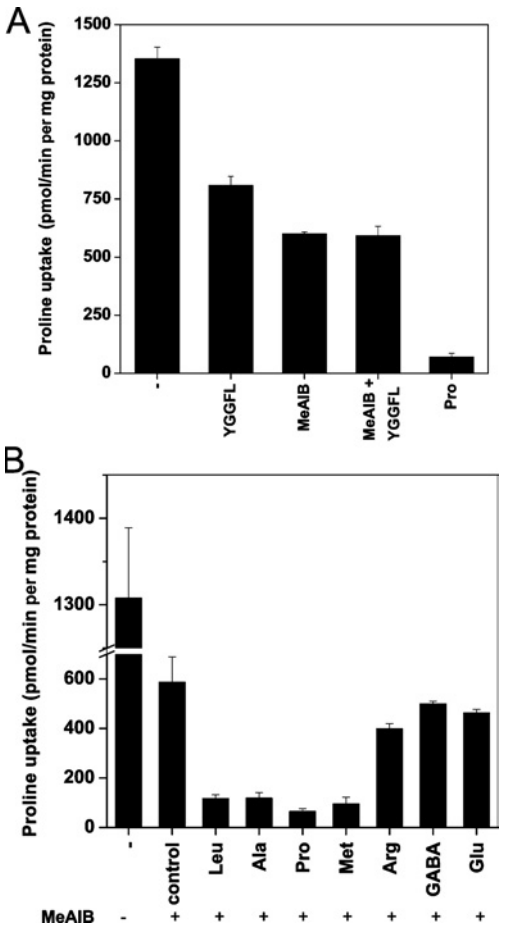

Figure 8 Proline uptake into cortical synaptosomes

Synaptosomes (20 μl) were added to 180 μl of transport buffer containing 50 μM [^{14}C]proline and incubated for 5 min at room temperature. (**A**) Uptake of 50 μM [^{14}C]proline was challenged with [leucine]enkephalin (YGGFL, 100 μM), MeAIB (10 mM) or a combination of the two compounds. As a control, [^{14}C]proline uptake was studied in the presence of 10 mM unlabelled proline (Pro) and in the absence of any competitor (−). The experiment was carried out three times using triplicate samples. (**B**) Uptake of 50 μM [^{14}C]proline was determined in the presence of 10 mM MeAIB to suppress the MeAIB-sensitive fraction of proline uptake (see **A**). The MeAIB-resistant uptake was challenged with addition of 10 mM unlabelled amino acids as indicated. The experiment was carried out three times using triplicate samples.

B^{0}AT2 is resistant to [leucine]enkephalin inhibition (Figure 1), we wondered whether a B^{0}AT2-like activity could also be detected in synaptosomes. Similar to neurons, proline uptake in synaptosomes was entirely Na^+-dependent. In contrast with cultured neurons, however, proline uptake was strongly inhibited by MeAIB and, to a similar extent, by [leucine]enkephalin (Figure 8A). Combining the two inhibitors did not increase inhibition, suggesting that MeAIB and [leucine]enkephalin inhibit the same transporter. To study the MeAIB-resistant (and [leucine]-enkephalin-resistant) proline uptake (approx. 40 % of total proline uptake), we subsequently characterized proline uptake in synaptosomes in the presence of 10 mM MeAIB. The MeAIB-resistant fraction of proline uptake was strongly inhibited by leucine, alanine, methionine and proline itself. Other amino acids which are not substrates of B^{0}AT2, such as arginine, GABA or glutamate, did not inhibit MeAIB-resistant proline uptake (Figure 8B). In summary, it seems that a transport activity matching the properties of B^{0}AT2 can be detected in both cultured neurons and cortical synaptosomes.

DISCUSSION

In the present study we identified the orphan neurotransmitter transporter v7-3 as a Na^+-dependent transporter for large neutral amino acids. Because of its functional similarity to B^{0}AT1 [20], we named it B^{0}AT2. We suggest that the orphan transporter branch of the SLC6 family should be renamed into the amino acid transporter branch (II), discriminating it from the amino acid transporter branch (I), which comprises two glycine transporters, the neuronal proline transporter PROT and the general amino acid transporter ATB$^{0,+}$ [5]. The Na^+-dependent amino acid transporters of the SLC6 family furthermore belong to a much larger family of Na^+-dependent nutrient amino acid transporters (NAT family) [26], with members found in bacteria [27], insects [26,28,29] and a variety of other lower and higher eukaryotes [26]. It appears that this family initially evolved to serve in amino acid uptake from nutrient sources in unicellular and multicellular organisms, whereas neurotransmitter transport is likely to be a more recent development.

Our results indicate that B^{0}AT2 mediates a 1:1 Na^+/amino acid co-transport as supported by the following evidence: (i) the transporter is Na^+-dependent and Cl^--independent; (ii) the Na^+-activation curves are hyperbolic; (iii) the transporter is electrogenic, translocating approx. one charge per substrate molecule; and (iv) protons are unlikely to participate in the transport mechanism and the pH-dependence is most probably caused by an exofacial modifier site. These properties match those of B^{0}AT1 [20], suggesting that both transporters have the same transport mechanism. Increasing the electrical driving force increased the apparent affinity of B^{0}AT2 for substrate and co-substrate. A possible explanation for this observation is that the negative membrane potential causes an increase of the local Na^+ concentration at its binding site (ion-well effect). An increase of the local Na^+ concentration also would decrease the proline $K_{0.5}$, thereby explaining the effect of the membrane potential on the apparent proline affinity. The mutual influence of substrate and co-substrate on each other's $K_{0.5}$ values suggests a possible interaction between substrate and co-substrate at the binding site. This view is supported by the recently published crystal structure of the prokaryotic SLC6-related transporter $LeuT_{Aa}$ from the bacterium *Aquifex aeolicus* [30], which has 26 % amino acid residues similar to, or identical with, those in mB^{0}AT2 (Figure 9, and Supplementary Figure 2 at http://www.BiochemJ.org/bj/393/bj3930421add.htm). The occurrence of highly conserved residues throughout the sequence allowed us to develop a topological model of mB^{0}AT2, which aligns well with the structure of the bacterial transporter (Figure 9). In particular, residues in helix 1 and helix 6, which form the substrate- and Na^+-binding sites of the bacterial transporter, are highly conserved. The loops and termini are significantly longer in the mammalian transporter and are not conserved. In the $LeuT_{Aa}$ structure, the carboxy group of the substrate leucine contributes to the coordination of the Na^+ ion. This overlapping binding site elegantly explains the mutual influence of substrate and co-substrate on each other's $K_{0.5}$ values. Na^+ will provide an improved binding site for leucine and vice versa. Notably, all but one residue implicated in substrate- and Na^+-binding in the bacterial transporter are fully conserved in B^{0}AT2. Also conserved are several residues that form the substrate binding pocket (helix 8) (accommodating leucine in both transporters) and the four residues that are proposed to form the cytosolic and extracellular gates.

Inhibition of proline transport by branched-chain amino acids is a unique property of B^{0}AT2. Other neuronal proline transporters such as PROT [24], PAT1/2 [31] and the system A isoforms SNAT1 and SNAT2 [32] do not accept large bulky neutral amino

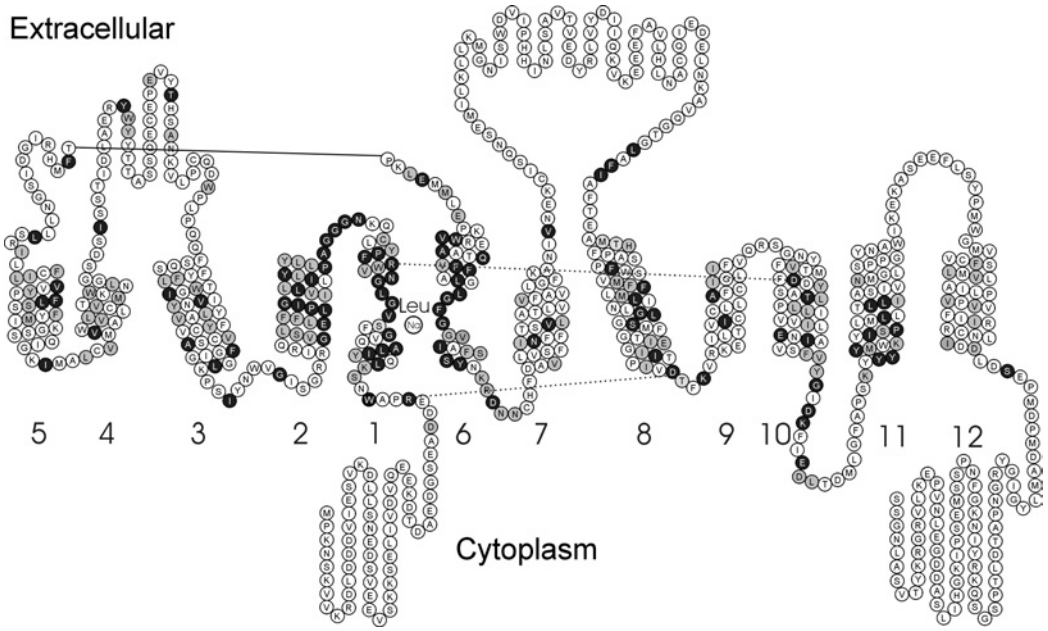

Figure 9 Topological model of mB^{0}AT2

A topological model of mB^{0}AT2 was derived by aligning the primary structure of mouse slc6 transporters with the primary structure of $LeuT_{Aa}$ from *Aquifex aeolicus* (NP_214423). The boundaries of the transmembrane regions were drawn in agreement with a similar alignment (shown in [30]). Residues that are identical with those of $LeuT_{Aa}$ in the alignment are shown in black, similar residues are shown in grey. Helices 1 and 6 are depicted next to each other because they form the substrate-binding site. Both helices are discontinuous, in line with the published structure. The proposed location of the binding sites for leucine (Leu), and Na^+ (Na) are indicated. The residues which may form the two gates of the transporter are connected by dotted lines. The solid line indicates the continuation of the primary structure in the topology model. The break had to be introduced because of the inverse assembly of helices 1–6.

acids as substrates. Inhibitors of these transporters, such as MeAIB (SNAT1/2), GABA (PAT1 and PAT2) and [leucine]-enkephalin (PROT), on the other hand, do not inhibit B^{0}AT2, therefore allowing discrimination of the different transport activities in cultured neurons and synaptosomes. In cultured neurons, we found little inhibition of proline uptake by GABA and MeAIB, excluding a significant contribution to proline uptake by SNAT1, SNAT2, PAT1 and PAT2. Although we found mRNAs of all four transporters, they appeared to be located in intracellular membranes and hence their transport activity was inaccessible. This notion is supported by previous studies showing that surface expression of SNAT1 and SNAT2 is suppressed by amino acids in the medium [33] and that PAT1 is mainly localized in intracellular membranes in neurons [34]. We found very little mRNA for PAT2, hence neurons may not express significant amounts of the protein. In contrast with the limited inhibition by MeAIB and GABA, a 100-fold excess of the B^{0}AT2 substrates leucine, methionine and AIB inhibited [^{14}C]proline uptake by approx. 75 %, which is the same extent of inhibition as exerted by unlabelled proline itself. Moreover, it excludes a significant contribution of the proline-specific transporter PROT, confirming that PROT is also mainly localized in intracellular membranes [35]. The properties of B^{0}AT2 are remarkably similar to the Na^+-dependent proline transport activity described in rat brain slices [36], which is inhibited by leucine, norleucine and norvaline. The situation appears to be different in synaptosomes. We confirmed that a significant fraction of proline uptake in synaptosomes is inhibited by [leucine]enkephalin and MeAIB [25]. Both compounds appear to inhibit the same transporter because their effect was not additive. MeAIB is commonly used to delineate system A. However, MeAIB also inhibits most proline transporters, such as PAT1 and IMINO, and is likely to inhibit PROT as well. The [leucine]enkephalin-resistant proline uptake (approx. 40 % of total uptake), in contrast, matched the properties of B^{0}AT2. As a result, it appears that synaptosomal proline uptake has two components, one attributable to PROT and the second to B^{0}AT2. It is worth noting that a [leucine]enkephalin-resistant fraction of synaptosomal proline uptake was noted previously [25] and was characterized as Cl^--independent, in line with the properties of B^{0}AT2.

The distribution of the neurotransmitter transporter v7-3 has been studied in some detail in rat brain by *in situ* hybridization [37]. Expression of the transporter was detected in neurons, but the distribution pattern was not compatible with any specific neurotransmitter, as seen by the presence of hybridization signals in dopaminergic neurons (substantia nigra), serotonergic neurons (raphe nuclei), noradrenergic neurons (locus coeruleus), glutamatergic neurons (hippocampus, olfactory bulb) and cholinergic neurons (motor neurons). This seemingly diffuse distribution can be explained by a role of B^{0}AT2 in the provision of neurotransmitter precursors. The nitrogen of leucine, for example, is efficiently transferred to α-oxoglutarate, thereby forming glutamate [1]. Isoleucine, methionine and valine can be metabolized to form succinyl-CoA and hence can act as precursors for glutamate biosynthesis. In motor neurons, methionine provides the methyl groups for acetylcholine biosynthesis [38,39]. Methionine is also a precursor of homocysteic acid, a glutamate analogue, which has been suggested as an excitatory amino acid in the brain [40]. The physiological role of proline in the brain is still ill-defined. Proline can be converted into glutamate, involving proline dehydrogenase and glutamate–semialdehyde dehydrogenase, but these enzymes appear to be associated with astrocytes [41], whereas PROT and B^{0}AT2 are expressed in neurons. The role of B^{0}AT2 in aminergic neurons remains to be defined.

In summary, it is likely that the major function of B^{0}AT2 is the transport of neurotransmitter precursors into neurons. The physiological role of neuronal proline accumulation remains to be determined.

This study was supported by grants from the Australian Research Council (ARC Discovery Project Grants DP 0208961 and DP0559104) and the National Health and Medical Research Council (Project Grant 224229) to S. B. L. K. B. carried out this work as a visiting student to the Australian National University.

REFERENCES

1 Yudkoff, M., Daikhin, Y., Nelson, D., Nissim, I. and Erecinska, M. (1996) Neuronal metabolism of branched-chain amino acids: flux through the aminotransferase pathway in synaptosomes. J. Neurochem. **66**, 2136–2145
2 Herrero, E., Aragon, M. C., Gimenez, C. and Valdivieso, F. (1983) Tryptophan transport into plasma membrane vesicles derived from rat brain synaptosomes. J. Neurochem. **40**, 332–337
3 O'Kane, R. L. and Hawkins, R. A. (2003) Na^+-dependent transport of large neutral amino acids occurs at the abluminal membrane of the blood–brain barrier. Am. J. Physiol. Endocrinol. Metab. **285**, E1167–E1173
4 Broer, S. (2002) Adaptation of plasma membrane amino acid transport mechanisms to physiological demands. Pflugers Arch. **444**, 457–466
5 Chen, N. H., Reith, M. E. and Quick, M. W. (2004) Synaptic uptake and beyond: the sodium- and chloride-dependent neurotransmitter transporter family SLC6. Pflugers Arch. **447**, 519–531
6 Nelson, N. (1998) The family of Na^+/Cl^- neurotransmitter transporters. J. Neurochem. **71**, 1785–1803
7 Broer, A., Klingel, K., Kowalczuk, S., Rasko, J. E., Cavanaugh, J. and Broer, S. (2004) Molecular cloning of mouse amino acid transport system B^0, a neutral amino acid transporter related to Hartnup disorder. J. Biol. Chem. **279**, 24467–24476
8 Kowalczuk, S., Broer, A., Munzinger, M., Tietze, N., Klingel, K. and Broer, S. (2005) Molecular cloning of the mouse IMINO system: an Na^+- and Cl^--dependent proline transporter. Biochem. J. **386**, 417–422
9 Takanaga, H., Mackenzie, B., Suzuki, Y. and Hediger, M. A. (2005) Identification of mammalian proline transporter SIT1 (SLC6A20) with characteristics of classical system IMINO. J. Biol. Chem. **280**, 8974–8984
10 Uhl, G. R., Kitayama, S., Gregor, P., Nanthakumar, E., Persico, A. and Shimada, S. (1992) Neurotransmitter transporter family cDNAs in a rat midbrain library: 'orphan transporters' suggest sizable structural variations. Mol. Brain Res. **16**, 353–359
11 Sakata, K., Shimada, S., Yamashita, T., Inoue, K. and Tohyama, M. (1999) Cloning of a bovine orphan transporter and its short splicing variant. FEBS Lett. **443**, 267–270
12 Farmer, M. K., Robbins, M. J., Medhurst, A. D., Campbell, D. A., Ellington, K., Duckworth, M., Brown, A. M., Middlemiss, D. N., Price, G. W. and Pangalos, M. N. (2000) Cloning and characterization of human NTT5 and v7-3: two orphan transporters of the Na^+/Cl^--dependent neurotransmitter transporter gene family. Genomics **70**, 241–252
13 Broer, S., Rahman, B., Pellegri, G., Pellerin, L., Martin, J. L., Verleysdonk, S., Hamprecht, B. and Magistretti, P. J. (1997) Comparison of lactate transport in astroglial cells and monocarboxylate transporter 1 (MCT 1) expressing *Xenopus laevis* oocytes: expression of two different monocarboxylate transporters in astroglial cells and neurons. J. Biol. Chem. **272**, 30096–30102
14 Broer, S. (2003) *Xenopus laevis* oocytes. Methods Mol. Biol. **227**, 245–258
15 Broer, S., Schneider, H. P., Broer, A., Rahman, B., Hamprecht, B. and Deitmer, J. W. (1998) Characterization of the monocarboxylate transporter 1 expressed in *Xenopus laevis* oocytes by changes in cytosolic pH. Biochem. J. **333**, 167–174
16 Brewer, G. J., Torricelli, J. R., Evege, E. K. and Price, P. J. (1993) Optimized survival of hippocampal neurons in B27-supplemented Neurobasal, a new serum-free medium combination. J. Neurosci. Res. **35**, 567–576
17 Lopez-Perez, M. J. (1994) Preparation of synaptosomes and mitochondria from mammalian brain. Methods Enzymol. **228**, 403–411
18 Brooks, D. E. and Norris-Jones, R. (1994) Preparation and analysis of two-phase systems. Methods Enzymol. **228**, 14–27
19 Thompson, J. D., Higgins, D. G. and Gibson, T. J. (1994) CLUSTAL W: improving the sensitivity of progressive multiple sequence alignment through sequence weighting, position-specific gap penalties and weight matrix choice. Nucleic Acids Res. **22**, 4673–4680
20 Bohmer, C., Broer, A., Munzinger, M., Kowalczuk, S., Rasko, J. E., Lang, F. and Broer, S. (2005) Characterization of mouse amino acid transporter B^0AT1 (slc6a19). Biochem. J. **389**, 745–751
21 Sonders, M. S. and Amara, S. G. (1996) Channels in transporters. Curr. Opin. Neurobiol. **6**, 294–302
22 Mackenzie, B. and Erickson, J. D. (2004) Sodium-coupled neutral amino acid (System N/A) transporters of the SLC38 gene family. Pflugers Arch. **447**, 784–795
23 Boll, M., Daniel, H. and Gasnier, B. (2004) The SLC36 family: proton-coupled transporters for the absorption of selected amino acids from extracellular and intracellular proteolysis. Pflugers Arch. **447**, 776–779
24 Fremeau, Jr, R. T., Caron, M. G. and Blakely, R. D. (1992) Molecular cloning and expression of a high affinity L-proline transporter expressed in putative glutamatergic pathways of rat brain. Neuron **8**, 915–926
25 Fremeau, Jr, R. T., Velaz-Faircloth, M., Miller, J. W., Henzi, V. A., Cohen, S. M., Nadler, J. V., Shafqat, S., Blakely, R. D. and Domin, B. (1996) A novel nonopioid action of enkephalins: competitive inhibition of the mammalian brain high affinity L-proline transporter. Mol. Pharmacol. **49**, 1033–1041
26 Boudko, D. Y., Kohn, A. B., Meleshkevitch, E. A., Dasher, M. K., Seron, T. J., Stevens, B. R. and Harvey, W. R. (2005) Ancestry and progeny of nutrient amino acid transporters. Proc. Natl. Acad. Sci. U.S.A. **102**, 1360–1365
27 Androutsellis-Theotokis, A., Goldberg, N. R., Ueda, K., Beppu, T., Beckman, M. L., Das, S., Javitch, J. A. and Rudnick, G. (2003) Characterization of a functional bacterial homologue of sodium-dependent neurotransmitter transporters. J. Biol. Chem. **278**, 12703–12709
28 Feldman, D. H., Harvey, W. R. and Stevens, B. R. (2000) A novel electrogenic amino acid transporter is activated by K^+ or Na^+, is alkaline pH-dependent, and is Cl^--independent. J. Biol. Chem. **275**, 24518–24526
29 Castagna, M., Shayakul, C., Trotti, D., Sacchi, V. F., Harvey, W. R. and Hediger, M. A. (1998) Cloning and characterization of a potassium-coupled amino acid transporter. Proc. Natl. Acad. Sci. U.S.A. **95**, 5395–5400
30 Yamashita, A., Singh, S. K., Kawate, T., Jin, Y. and Gouaux, E. (2005) Crystal structure of a bacterial homologue of Na^+/Cl^--dependent neurotransmitter transporters. Nature (London) **437**, 215–223
31 Boll, M., Foltz, M., Rubio-Aliaga, I., Kottra, G. and Daniel, H. (2002) Functional characterization of two novel mammalian electrogenic proton-dependent amino acid cotransporters. J. Biol. Chem. **277**, 22966–22973
32 Mackenzie, B., Schafer, M. K., Erickson, J. D., Hediger, M. A., Weihe, E. and Varoqui, H. (2003) Functional properties and cellular distribution of the system A glutamine transporter SNAT1 support specialized roles in central neurons. J. Biol. Chem. **278**, 23720–23730
33 Ling, R., Bridges, C. C., Sugawara, M., Fujita, T., Leibach, F. H., Prasad, P. D. and Ganapathy, V. (2001) Involvement of transporter recruitment as well as gene expression in the substrate-induced adaptive regulation of amino acid transport system A. Biochim. Biophys. Acta **1512**, 15–21
34 Rubio-Aliaga, I., Boll, M., Vogt Weisenhorn, D. M., Foltz, M., Kottra, G. and Daniel, H. (2004) The proton/amino acid cotransporter PAT2 is expressed in neurons with a different subcellular localization than its paralog PAT1. J. Biol. Chem. **279**, 2754–2760
35 Renick, S. E., Kleven, D. T., Chan, J., Stenius, K., Milner, T. A., Pickel, V. M. and Fremeau, Jr, R. T. (1999) The mammalian brain high-affinity L-proline transporter is enriched preferentially in synaptic vesicles in a subpopulation of excitatory nerve terminals in rat forebrain. J. Neurosci. **19**, 21–33
36 Balcar, V. J., Johnston, G. A. and Stephanson, A. L. (1976) Transport of L-proline by rat brain slices. Brain Res. **102**, 143–151
37 Inoue, K., Sato, K., Tohyama, M., Shimada, S. and Uhl, G. R. (1996) Widespread brain distribution of mRNA encoding the orphan neurotransmitter transporter v7-3. Mol. Brain Res. **37**, 217–223
38 Vance, J. E. and Vance, D. E. (2004) Phospholipid biosynthesis in mammalian cells. Biochem. Cell Biol. **82**, 113–128
39 Blusztajn, J. K., Liscovitch, M., Mauron, C., Richardson, U. I. and Wurtman, R. J. (1987) Phosphatidylcholine as a precursor of choline for acetylcholine synthesis. J. Neural Transm. Suppl. **24**, 247–259
40 Thompson, G. A. and Kilpatrick, I. C. (1996) The neurotransmitter candidature of sulphur-containing excitatory amino acids in the mammalian central nervous system. Pharmacol. Ther. **72**, 25–36
41 Thompson, S. G., Wong, P. T., Leong, S. F. and McGeer, E. G. (1985) Regional distribution in rat brain of 1-pyrroline-5-carboxylate dehydrogenase and its localization to specific glial cells. J. Neurochem. **45**, 1791–1796

Received 4 August 2005/23 August 2005; accepted 26 September 2005
Published as BJ Immediate Publication 26 September 2005, doi:10.1042/BJ20051273